

# A High Sensitivity and Low-Cost Polycarbonate (PC)-based Biosensor

Yu-Shan Chen and Gou-Jen Wang\*

\*Graduate Institute of Biomedical Engineering, National Chung-Hsing University, Taiwan  
gjwang@dragon.nchu.edu.tw

**Abstract**—This study integrates the techniques of nano electroforming, hot embossing, and electrochemical deposition to develop a disposable, low cost, and high sensitivity nanostructure biosensor. A modified anodic aluminum oxide (AAO) barrier-layer surface is used as the template for nickel thin film deposition. After etching the AAO template off, a 3D mold of the concave nano structure array is created. The fabricated 3D nickel mold is further used for replica molding of a nano-structure polycarbonate (PC) substrate by hot embossing. An Au thin film is then sputtered on the PC substrate to form the electrode followed by the deposition of an orderly and uniform gold nanoparticle (GNP) layer on the 3D Au electrode using electrochemical deposition. Finally, silver nanoparticles (SNP) are deposited on the uniformly deposited GNPs to enhance the conductivity of the sensor. Electrochemical impedance spectroscopy (EIS) analysis is then used to detect the concentration of the target element. The sensitivity of the proposed scheme on the detection of the dust mite antigen Der p2 can reach 0.1pg/ml.

**Keywords**- nano electroforming, nano-structure polycarbonate (PC) substrate, gold nanoparticles, silver nanoparticles, EIS analysis

## I. INTRODUCTION

The current trend for point of care device development requires that a device be low cost, sensitive, specific, easy to use, rapid and robust, and disposable, as well as having a small sample requirement. This is especially the case for people who live in developing countries where even common tests are not affordable and the fundamental infrastructure is often not available [1-3]. A variety of microfluidic devices such as the micro total analysis system ( $\mu$ TAS) have been developed which partially meet these demands [4-7]. However, the requirement of lithographic equipment and the relatively high cost of such devices can prove to place limitations for mass production and general applications.

Microfluidic paper-based analytical devices ( $\mu$ PADs) as initially proposed by Whitesides group can be good alternatives to satisfy the low cost and ease of use requirements of modern point-of-care diagnostic devices [8-10]. A  $\mu$ PAD generally consists of a paper-based microfluidic testing platform based on patterned channels on hydrophilic paper delimited by partitions of hydrophobic material and a light reflectance detector for quantitative colorimetric detection of target analytes at the test zone. Methods for paper patterning include photolithography [8,11], plotter printing of

PDMS patterns in paper [12], inkjet printing [13,14], and wax printing [15,16]. A simple reflectance detection device such as a desktop scanner or a digital camera is quite adequate for use with a  $\mu$ PAD. Other detection methods such as quantitative fluorescence and absorbance measurements obtained using a microplate reader [17], electrochemistry [18-20], or electrochemiluminescence [21] can also be implemented for the quantitative detection of the target analytes. The  $\mu$ PEDs, although still in their infancy, have proven to be a promising solution for simple and low-cost quantitative detection of biological and inorganic species in aqueous solutions. However, their relatively low sensitivity may limit their applications for the detection of rare molecules. A low-cost diagnostic device, with high sensitivity, is still desired for precise detection of low levels of species in biological samples, including bodily fluids.

Nanomaterials, which can provide a substantially larger surface area than that of bulk material or thin films, have been used to either simplify the readout or magnify the detection signal of a diagnostic device [22-24]. Several nanomaterial-based devices have also been approved by the FDA for in vitro diagnosis [25-28].

This study demonstrates the integration of nano electroforming, hot embossing, electrochemical deposition techniques for the fabrication of a polycarbonate (PC) based biosensor platform. The key component in this PC-based platform is a GNP-deposited nano-structured PC substrate which serves as the transducer for the detection of the target analytes by binding to it. The nano-structure PC substrates can be replicated using a nickel mold by means of nano hot embossing or nano injection molding. This makes the platform disposable and low cost. In addition, the high surface to volume ratio of the nano-structure PC substrate and the uniformly deposited GNPs allows the attachment of many more analytes to the transducer which in turn means considerable enhancement of the sensitivity. In this study, the detection of the dust mite antigen Der p2 is carried out using electrochemical impedance spectroscopy (EIS) analysis to demonstrate the performance of the proposed PC-based biosensor scheme.

## II. EXPERIMENTAL SECTION

### A. PC-based Transducer Fabrication

Figure 1 shows a schematic illustration of the proposed PC-based biosensor design. It consists of a PC substrate with a nano-hemisphere array, a gold thin film sputtered on the PC substrate to form the electrode, gold nanoparticles uniformly deposited on the film, and smaller silver nanoparticles deposited on the GNPs. The sequential fabrication processes include: fabrication of a nano-structured PC substrate; deposition of an Au thin film; annealing; electrochemical deposition of Au nanoparticles; and electrochemical deposition of Ag nanoparticles.

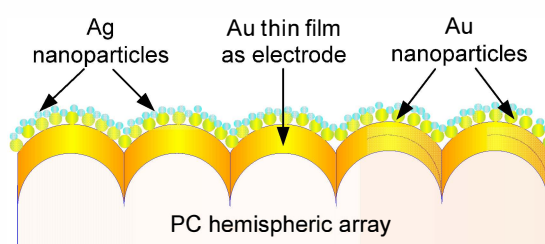


Fig. 1. Schematic illustration of the proposed PC-based biosensor.

#### (1) Fabrication of a nano-structured PC substrate

The nano-structured PC substrate is hot-embossed using a nickel replica mold. The fabrication procedures of the nano replica mold are briefly described as follows. A modified anodic aluminum oxide (AAO) barrier-layer surface is used as the master mold for nickel thin film deposition. After etching off the AAO template, a 3D replica of the concave nanostructure array can be obtained.

The nano-structured PC substrates were produced by Leadoptical Co., Ltd., Taichung, Taiwan. Leadoptical specializes in microlens array fabrication. Since the glass transition temperature ( $T_g$ ) of the PC used is  $120^\circ\text{C}$ , the embossing temperature is set at  $150^\circ\text{C}$ . After holding for 50 sec, a cooling process at  $100^\circ\text{C}$  for 180 sec is carried out.

#### (2) Deposition of Au thin film

An Au thin film electrode is deposited on the hemispheric array of the PC substrate using radio frequency (RF) magnetron sputtering. The deposition is conducted under a  $4.0 \times 10^{-3}$  torr pressure at room temperature with a 20 sccm argon injection and an 80 W power lasting for 1.5 min. This creates a 30 nm thick Au thin film.

#### (3) Annealing

To further refine the surface structure of the Au thin film electrode and make it homogeneous, an annealing process is employed. The sequential annealing procedures include: heating the sample to  $120^\circ\text{C}$  at a rate of  $5^\circ\text{C}/\text{min}$ , maintaining that temperature for 60 min, followed by cooling the sample in open air to room temperature.

#### (4) Packaging

To ensure the uniformity of the sensing area and prevent other solutions from getting in touch with the sample, precise packaging before electrochemical depositing of Au nanoparticles is needed. The packaging procedures are described as follows:

(i) Prepare a  $2.5 \times 2.5$  cm<sup>2</sup> square parafilm.

(ii) Make a  $\phi=6$  mm hole in the center of the parafilm.

(iii) Daub a thin layer of epoxy on the bottom surface of the parafilm square, followed by bonding of the parafilm to the Au film deposited PC substrate to enclose the sensing area of the device.

(iv) Package the device using silica gel to ensure air tightness.

#### (4) Deposition of Au nanoparticles

The electrochemical deposition is processed by an SP-150 an electrochemical analyzer (EC-Lab, USA). The packaged

sample is placed at the working electrode (WE), with the Au thin film serving as the electrode. The counter electrode and the reference electrode (RE) are a Pt film and an Ag/AgCl electrode, respectively. The deposition processes are described below.

#### (i) Electrolyte preparation:

The electrolyte is prepared by dissolving 1 mL of 0.02 M HAuCl<sub>4</sub> (Aldrich Inc.) solution in 39 mL of deionized water.

#### (ii) Reducing potential measurement:

The cyclic voltammetric method is conducted using the SP-150 to examine the reduction potential of the HAuCl<sub>4</sub> solution. The scanning range is set to be between  $-0.8$  V and  $+0.8$  V. Three reducing peaks, at  $0.8$  V,  $-0.2$  V, and  $-0.8$  V, respectively, are detected, where  $-0.8$  V denotes the reducing peak of a monovalence Au ion. Several experiments with reducing potentials set around  $-0.8$  V are conducted. The results indicate that  $-0.7$  V is a more suitable reducing potential for the HAuCl<sub>4</sub> solution used in this study.

#### (iii) Electrochemical deposition:

The electrochemical deposition is processed under a DC  $-0.7$  V electric potential at room temperature, lasting for 180 sec. Several experiments with different deposition durations are carried out. It is found that 180 sec can perform better deposition of GNP.

#### (5) Deposition of Ag nanoparticles

Due to its extra high electric and thermal conductivity, silver has been widely applied to micro/nano systems to enhance conductivity. In this study, silver nanoparticles are produced using the Meisel rodex method [29]. Ag nanoparticles are then electrochemically deposited on the Au nanoparticles to further increase the device's conductivity. The deposition processes are described below.

#### (i) Electrolyte preparation:

The electrolyte for producing Ag nanoparticles is a mixture of 1mM water bathed NaBH<sub>4</sub> and 1mM AgNO<sub>3</sub>. Canary yellow Ag nanoparticles can be synthesized by stirring the electrolyte at  $40^\circ\text{C}$  for 2 min. Continuing stirring for 1 hr is essential to prevent aggregation of the Ag nanoparticles.

#### (ii) Reducing potential measurement:

The reducing potential for better reduction of Ag ions is detected to be  $-0.4$  V through the cyclic voltammetric procedures same as the measurement of the reducing potential for the HAuCl<sub>4</sub> solution.

#### (iii) Electrochemical deposition:

Electrochemical deposition of Ag nanoparticles was conducted by the application of a DC  $-0.4$  V electric potential for 150 sec at room temperature.



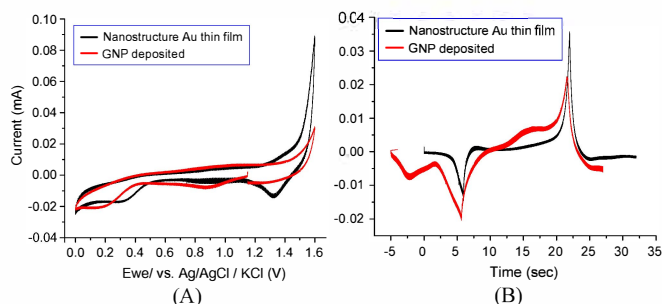


Fig4. CVs and I-t curves transformed from the CVs for the film before deposition of the nanostructure Au thin film and the GNP deposited electrodes.

PC/Au/GNP electrode are estimated to be 16.51 and 53.90  $\mu\text{C}$ , respectively. Since the charges required to form AuO per 1  $\text{cm}^2$  of Au electrode is 386  $\mu\text{C}$ , the effective areas of the Au thin film before GNP nanostructure deposition and the PC/Au/GNP electrode are calculated to be 0.043 (16.51  $\mu\text{C}/386 \mu\text{C}$ ) and 0.14 (53.90  $\mu\text{C}/386 \mu\text{C}$ )  $\text{cm}^2$ , respectively. The effective area is enhanced 3.26-fold due to the deposition of GNPs.

### C. Electrochemical Impedance Spectroscopy Analysis Results

The EIS analysis results obtained using an SP-150 electrochemical analyzer are presented in Figure 5. Figure 5(A) shows the Nyquist plots for a GNP deposited electrode, an electrode after the anti-dust mite monoclonal IgG is bound to the NHS-EDC, and electrodes after the Der p2 (with various concentrations) are immobilized for the anti-dust mite monoclonal IgG. The diameter of each individual semicircular EIS curve in Figure 5(A) represents the charge transfer resistance of the electrode with respect to this specific EIS analysis. Figure 5(A) reveals that the charge transfer resistance for each individual electrode increases with an increase in the Der p2 concentration. In other words, the impedance of the Der p2 binding device increases with an increase in the Der p2 concentration. The EIS analysis results can be modeled by the Randles's equivalent circuit shown in the inset to Figure 5(A).

The total impedance in the Randles's equivalent circuit is composed of the electrolyte resistance ( $R_s$ ), the charge transfer resistance ( $R_{et}$ ), and the double layer capacitance ( $C_{dl}$ ). Since  $R_s$  represents the bulk properties of the electrolyte solution, it is unrelated to the chemical reactions coming about at the electrode interface. The values of  $R_{et}$  and  $C_{dl}$  change with the substance bonded onto the electrode surface. Table 1 presents the fitting parameters for the equivalent circuit model of the PC-based biosensor corresponding to the Nyquist plots in Figure 5(A), in which,  $\Delta R_{et}$  denotes the different levels of resistance between the electrode in the individual SAM stage and the IgG bonding electrode. As tabulated in Table 1, the value of each  $R_s$  is much smaller, and can be neglected when compared with its corresponding  $R_{et}$  value. Hence, the Randles's equivalent circuit can be simplified as follows:

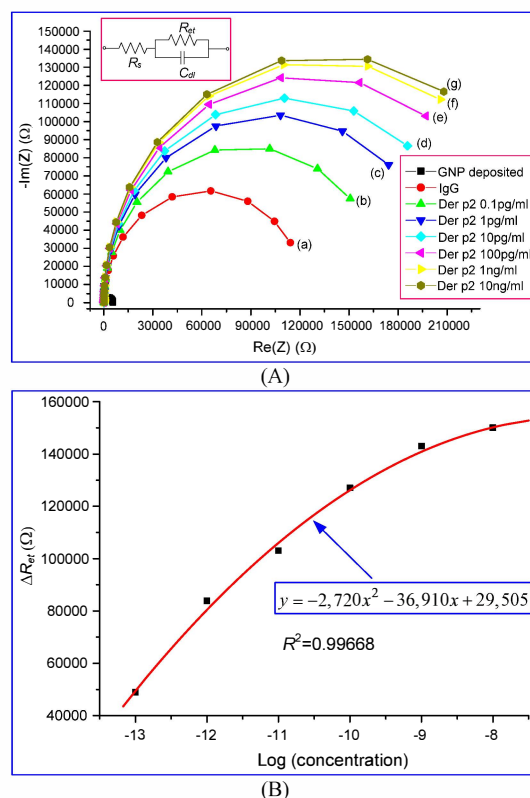


Fig.5. EIS analysis results: (A) Impedance plots for Der p2 at various concentrations: (a) IgG, (b)  $10^{-13}$ g/ml, (c)  $10^{-12}$ g/ml, (d)  $10^{-11}$ g/ml, (e)  $10^{-10}$ g/ml, (f)  $10^{-9}$ g/ml, (g)  $10^{-8}$ g/ml; (B)  $\Delta R_{et}$  as a function of the logarithmic concentration of Der p2 for the proposed PC-based biosensor.

TABLE I. FITTING PARAMETERS FOR THE RANDES'S EQUIVALENT CIRCUIT

	GNP	IgG	0.1 pg	1 pg	10 pg	100 pg	1 ng	10 ng
$R_{et}$ ( $10^5 \Omega$ )	0.053	1.24	1.73	2.07	2.26	2.51	2.67	2.73
$R_s$ ( $\Omega$ )	185	181	178	179	181	181	181	180
$C_{dl}$ ( $10^{-6}$ F)	3.95	3.73	3.51	3.35	3.38	3.31	3.24	3.26
$\Delta R_{et}$ ( $10^5 \Omega$ )			0.49	0.84	1.03	1.27	1.43	1.50

$$Z(\omega) = \frac{R_{et}}{1 + \omega^2 R_{et}^2 C_{dl}^2} - j \frac{\omega R_{et}^2 C_{dl}}{1 + \omega^2 R_{et}^2 C_{dl}^2} \quad (1)$$

$$= R + jX$$

As expressed in Eq. (2), both  $R_{et}$  and  $C_{dl}$  affect the impedance plot. However, Table 1 shows that the difference in  $R_{et}$  between the electrode for the individual SAM stage and the GNP deposited electrode is more substantial when compared with the change of  $C_{dl}$ . Hence,  $\Delta R_{et}$  can be used as the parameter to relate the sensor response with different analyte concentrations.

Figure 5(B) shows  $\Delta R_{et}$  as a function of the logarithmic concentration of Der p2 for the proposed PC-based nanobiosensor. The sensor response is well fitted by a conic

section with  $R^2=0.99668$ . The detection limit is around 0.1pg/ml as indicated by curve (a) in Figure 5(A). A dynamic range of up to 10 ng/ml (curve (g) in Figure 5(A)) is also presented. When the  $\Delta R_{et}$  of a desired Der p2 solution is detected, the concentration of Der p2 can be determined by this standard regression curve.

A test sample of 1pg/ml is used for further verification. The  $\Delta R_{et}$  of the test sample is measured to be  $8.27 \times 10^4 \Omega$ . The logarithmic concentration of the test sample is calculated to be -11.8 using the standard regression curve. It is only 1.7% off the real value of -12.

It is presumed that the uniformly distributed Au nanoparticles on the hemispheric array enable the MUA molecules to reach individual gold nanoparticles; therefore, the sequential bindings of EDC/NHS molecules and IgG molecules are thus increased. Hence, the effective binding between Der p2 and IgG can be enhanced. As a result, the sensitivity of the sensor is considerably enhanced. The proposed low-cost and high sensitivity PC-based nanobiosensor can be useful for the rapid detection of rare molecules in an analyte.

#### IV. CONCLUSIONS

In this study, we have designed a low-cost and highly sensitive PC-based nanostructured biosensor. The sequential synthesis processes of the biosensor include: fabrication of a nano-structured PC substrate; deposition of an Au thin film; annealing; electrochemical deposition of Au nanoparticles, and electrochemical deposition of Ag nanoparticles. The sensing limit and dynamic range of the proposed design for Der p2 detection are investigated using EIS analysis and found to be 0.1 pg/ml and 10 ng/ml, respectively. It is presumed that the uniformly distributed Au nanoparticles on the hemispheric array enable the MUA molecules to reach individual gold nanoparticles; thereby increasing the sequential bindings of EDC/NHS molecules and IgG molecules. Hence the effective binding between Der p2 and IgG can be enhanced, resulting in the sensitivity of the sensor being enhanced considerably. Fluorescence analysis results obtained using EGFP further indicate that the high sensitivity of the proposed PC-based nanobiosensor can be attributed to the intensity and uniformity of the Au nanoparticles on the sensor. The proposed low-cost and high sensitivity sensor can be useful for the rapid detection of rare molecules in an analyte.

In future work, the PC-based biosensor will be integrated into the conventional printed circuit board (PCB) fabrication process to produce a final product. Mass production tasks will be conducted. A portable EIS device is currently being designed and fabricated for fast and low-cost detection.

#### ACKNOWLEDGMENT

The authors would like to offer their thanks to the Department of Health of Taiwan for their financial support of this research under grant number DOH100-TD-N-111-006.

#### REFERENCES

- [1] S. K. Sia and L. J. Kricka, "Microfluidics and point-of-care testing," *Lab Chip*, vol. 8, pp. 1982-1983, 2008.
- [2] C. D. Chin, V. Linder, and S. K. Sia, "Lab-on-a-chip devices for global health: past studies and future opportunities," *Lab Chip*, vol. 7, pp. 41-57, 2007.
- [3] P. Yager, T. Edwards, E. Fu, K. Helton, K. Nelson, M. R. Tam, and B. H. Weigl, "Microfluidic diagnostic technologies for global public health," *Nature*, vol. 442, pp. 412-418, 2006.
- [4] Y. C. Lim, A. Z. Kouzani, W. Duan, "Lab-on-a-chip: a component view," *Microsyst. Technol.*, vol. 16, pp.1995-2015, 2010.
- [5] S. Haeblerle and R. Zengerle, "Microfluidic platforms for lab-on-a chip applications," *Lab Chip*, vol. 7, pp. 1094-1110, 2007.
- [6] A. G. Crevillen, M. Pumera, M. C. Gonzalez, A. Escarpa, "Towards lab-on-a-chip approaches in real analytical domains based on microfluidic chips/electrochemical multi-walled carbon nanotube platforms," *Lab Chip*, vol. 9, pp. 346-353, 2009.
- [7] Y. F. Lee, K. Y. Lien, H. Y. Lei, and G. B. Lee, "An integrated microfluidic system for rapid diagnosis of dengue virus infection," *Biosens. Bioelectron.* vol. 25, pp. 745-752, 2009.
- [8] A. W. Martinez, S. T. Phillips, M. J. Butte, and G. M. Whitesides, "Patterned paper as a platform for inexpensive, low-volume, portable bioassays," *Angew. Chem., Int. Ed.*, vol. 46, pp.1318-1320, 2007.
- [9] A. W. Martinez, S. T. Phillips, E. Carrilho, S. W. Thomas III, H. Sindi, and G. M. Whitesides, "Simple telemedicine for developing regions: camera phones and paper-based microfluidic devices for real-time, off-site diagnosis," *Anal. Chem.*, vol. 80, pp. 3699-3707, 2008.
- [10] A. W. Martinez, S. T. Phillips, and G. M. Whitesides, "Diagnostics for the developing world: microfluidic paper-based analytical devices," *Anal. Chem.*, vol. 82, pp. 3-10, 2010.
- [11] A. W. Martinez, S. T. Phillips, B. J. Wiley, M. Gupta, and G. M. Whitesides, "FLASH: A rapid method for prototyping paper-based microfluidic devices," *Lab Chip*, vol. 8, pp. 2146-2150, 2008.
- [12] D. A. Bruzewicz, M. Reches, and G. M. Whitesides, "Low-cost printing of poly (dimethylsiloxane) barriers to define microchannels in paper," *Anal. Chem.*, vol. 80, pp. 3387-3392, 2008.
- [13] K. Abe, K. Suzuki, and D. Citterio, "Inkjet-printing microfluidic multianalyte chemical sensing paper," *Anal. Chem.*, vol. 80, pp. 6928-6934, 2008.
- [14] X. Li, J. Tian, G. Garnier, and W. Shen, "Fabrication of paper-based microfluidic sensors by printing," *Colloids and Surfaces B: Biointerfaces*, vol. 76, pp. 564-570, 2010.
- [15] Y. Lu, W. Shi, J. Qin, and B. Lin, "Fabrication and characterization of paper-based microfluidics prepared in nitrocellulose membrane by wax printing," *Anal. Chem.*, vol. 82, pp. 329-335, 2010.
- [16] E. Carrilho, A. W. Martinez, and G. M. Whitesides, "Understanding wax printing: a simple micropatterning process for paper-based microfluidics," *Anal. Chem.*, vol. 81, pp. 7091-7095, 2009.
- [17] E. Carrilho, S. T. Phillips, S. J. Vella, A. W. Martinez, G. M. Whitesides, "Diagnostics for the developing world: microfluidic paper-based analytical devices," *Anal. Chem.*, vol. 81, pp. 5990-5998, 2009.
- [18] W. Dungchai, O. Chailapakul, and C. S. Henry, "Electrochemical detection for paper-based microfluidics," *Anal. Chem.*, vol.81, pp. 5821-5826, 2009.
- [19] Z. Nie, C. A. Nijhuis, J. Gong, X. Chen, A. Kumachev, A. W. Martinez, M. Narovlyansky, and G. M. Whitesides, "Electrochemical sensing in paper-based microfluidic devices," *Lab Chip*, vol. 10, pp. 477-483, 2010.
- [20] Z. Nie, F. Deiss, X. Liu, O. Akbulut, and G. M. Whitesides, "Integration of paper-based microfluidic devices with commercial electrochemical readers," *Lab Chip*, vol. 10, pp. 3163-3169, 2010.
- [21] J. L. Delaney, C. F. Hogan, J. Tian, and W. Shen, "Electrogenerated chemiluminescence detection in paper-based microfluidic sensors," *Anal. Chem.*, vol. 83, pp. 1300-1306, 2011.
- [22] Y. H. Yun, A. Bange, W. R. Heineman, H. B. Halsall, V. N. Shanov, Z. Dong, S. Pixley, M. Behbehani, A. Jazieh, Y. Tu, D. K. Y. Wong, A. Bhattacharya, and M. J. Schulz, "A nanotube array immunosensor for direct electrochemical detection of antigen-antibody binding," *Sensors and Actuators B*, vol. 123, pp. 177-182, 2007.
- [23] J. Huang, G. Yang, W. Meng, L. Wu, A. Zhu, X. Jiao, "An electrochemical impedimetric immunosensor for label-free detection of

- campylobacter jejuni in diarrhea patients' stool based on O-carboxymethylchitosan surface modified Fe<sub>3</sub>O<sub>4</sub> nanoparticles," *Biosens. Bioelectron.* vol. 40, pp. 893-896, 2009.
- [24] J. J. Tsai, I. J. Bau, H. T. Chen, Y. T. Lin, and G. J. Wang, "A novel nanostructured biosensor for the detection of the dust mite antigen Der p2," *Inter. J. Nanomedicine*, vol. 6, pp 1-8, 2011.
- [25] G. A. Posthuma-Trumpie, J. Korf J, and A. V. van Amerongen, "Lateral flow immunoassay: its strengths, weaknesses, opportunities and threats: a literature survey," *Anal. Bioanal. Chem.* Vol. 393, pp. 569-82, 2009.
- [26] J. M. Nam, C. S. Thaxton, C. A. Mirkin, "Nanoparticle-based bio-bar codes for the ultrasensitive detection of proteins," *Science*, vol. 301, pp. 1884-1886, 2003.
- [27] Lefferts JA, Jannetto P, Tsongalis GJ. Evaluation of the Nanosphere Verigene System and the Verigene F5/F2/MTHFR Nucleic Acid Tests. *Exp Mol Pathol* 2009;87:105-8.
- [28] C. S. Thaxton, R. Elghanian, and A. D. Thomas, "Nanoparticle-based bio-barcode assay redefines undetectable PSA and biochemical recurrence after radical prostatectomy," *Proc Natl Acad Sci USA*, vol. 106, pp.18437-18442, 2009.
- [29] J. Gehl, T. H. Sorensen, K. Nielsen, P. Raskmark, S. L. Nielsen, T. Skovsgaard, and L. M. Mir, "In vivo electroporation of skeletal muscle: Threshold, efficacy and relation to electric field distribution," *Biochimica et Biophysica Acta*, vol. 1428, pp. 233-240, 1999.
- [30] S. Hrapovic, Y. Liu, K. B. Male, and J. H. T. Luong, "Electrochemical biosensing platforms using platinum nanoparticles and carbon nanotubes," *Anal. Chem.*, vol. 76, pp. 1083-1088, 2004.